Signal Processing 152 (2018) 63–68

Contents lists available at ScienceDirect

Signal Processing

journal homepage: www.elsevier.com/locate/sigpro

Short communication

Transmit design and DOA estimation for wideband MIMO system with colocated nested arrays☆

Linlin Mao[a,1,*], Hongbin Li[b], Qunfei Zhang[a]

[a] School of Marine Science and Technology, Northwestern Polytechnical University, Xi'an 710072, China
[b] Department of Electrical and Computer Engineering, Stevens Institute of Technology, Hoboken, NJ 07030, USA

ARTICLE INFO

Article history:
Received 26 December 2017
Revised 15 April 2018
Accepted 16 May 2018
Available online 19 May 2018

Keywords:
Nested array
Wideband multiple-input multiple-output (MIMO) system
Transmit scheme
Direction of arrival (DOA) estimation
Degrees of freedom (DOF)

ABSTRACT

We consider transmit design and direction-of-arrival (DOA) estimation for a wideband multiple-input multiple-output (MIMO) system equipped with a colocated nested array for both transmit and receive. We present a new transmit scheme which separates the transmitted waveforms in the frequency domain, and allows us to form a sum coarray in the wideband case. Based on the proposed scheme, two coherent DOA estimation methods which construct focusing matrices from the difference coarray of the MIMO virtual array are presented to take full advantage of the degrees of freedom (DOF) and improve the accuracy of DOA estimation. Simulation results illustrate that the proposed system exhibits better performance than several competing configurations.

1. Introduction

Multiple-input multiple-output (MIMO) system has recently become an active research area due to its potential to provide higher spatial resolution, better parameter identifiability, greater flexibility in the beampattern design and more degrees of freedom (DOF) than its phased-array counterpart [1–6]. Most exiting works are focused on narrowband MIMO systems. Meanwhile, wideband MIMO technologies [7–9], which provide more target information and are less sensitive to active and passive interferences than their narrowband counterpart, are needed in a range of applications from high range resolution (HRR) radar, medical imaging, to underwater sonar systems.

Wideband MIMO sensing problems including waveform design (e.g., [8]) and receive beamforming/detection (e.g., [7,9]) have been addressed in literatures though not extensively. Wideband MIMO design has some unique challenges. In particular, the time delay cannot be neglected for the wideband case, which makes it more difficult to perform matched filtering directly. The authors of [7] proposed a time-domain method based on smearing filter banks, which allows to form MIMO virtual arrays in the broadband case but with some resolution loss. A frequency-domain approach for wideband MIMO radar was presented in [9] that decomposes the received wideband signal into multiple narrowband components, which are processed by narrowband beamforming/detection techniques followed by combining. However, their approach is based on the receive aperture processing, and cannot take advantage of the virtual array of the system. In general, there are few works addressing how to efficiently separate the transmit signals at the receive side and construct a virtual sum coarray to seek more DOF in the frequency domain.

Recently, nested array (NA) constructed by combining two or more uniform liner arrays (ULAs) has received considerable attention. Specifically, [10] proposed an NA based on the concept of difference coarray (DC), which can realize significantly more DOF and higher resolution performance in the passive sensing scenario.

In order to seek benefits such as additional DOF and higher resolution, we consider a wideband MIMO system using an NA for both transmit and receive. Transmit subaperturing using a colocated NA was recently introduced in [11] for a narrowband system. However, the integration of NA for wideband MIMO sensing as well as the related signal design have not been considered. In this work, we propose a new transmit scheme for wideband MIMO system so that the signals from different antennas can be easily separated in the frequency domain. Based on the proposed scheme, wideband NA processing techniques are presented to take full advantage of

☆ This work was supported in part by the National Natural Science Foundation of China under Grants 61531015 and 61501374.

* Corresponding author.
E-mail addresses: maple3511@mail.nwpu.edu.cn (L. Mao), hongbin.li@stevens.edu (H. Li), zhangqf@nwpu.edu.cn (Q. Zhang).

[1] This work is completed during her visit to the Department of Electrical and Computer Engineering, Stevens Institute of Technology, Hoboken, NJ 07030 USA.

https://doi.org/10.1016/j.sigpro.2018.05.014
0165-1684/

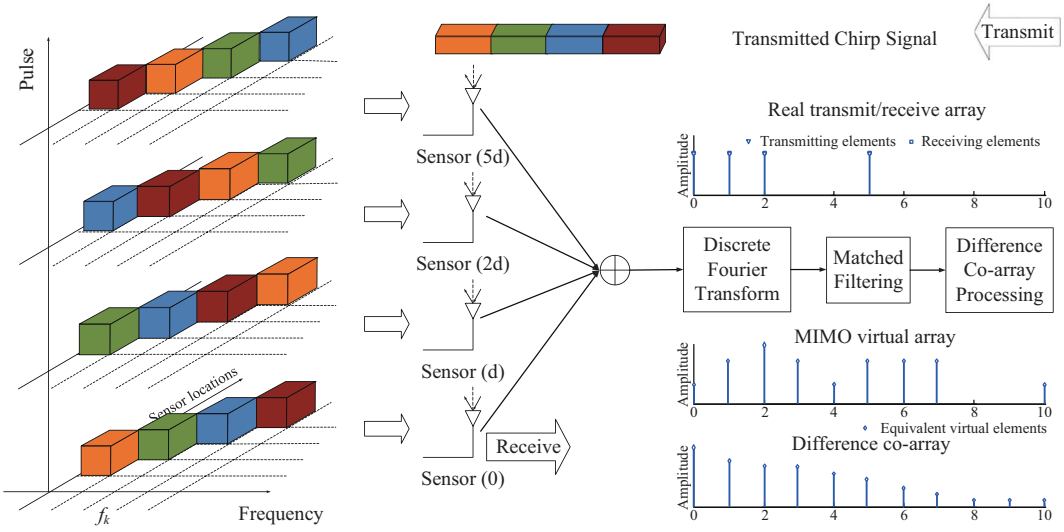

Fig. 1. Proposed wideband MIMO transmit and receive scheme with $N = 4$ antennas.

the DOF and improve the accuracy of direction of arrival (DOA) estimation.

2. Problem formulation

Consider a colocated omni-directional MIMO system consisting of M antennas with a nested array used for both transmit and receive. These M antennas form an optimal two-level nested array, which is a concatenation of an inner ULA with $J = \lfloor \frac{M}{2} \rfloor$ elements, and an outer ULA with $L = M - J$ elements. The spacing between two adjacent elements of the inner array is d, while the counterpart for the outer array is $(J+1)d$. The corresponding sensor locations are given by the union of the sets $S_{\text{in}} = \{jd, j = 0, 1, \ldots, J-1\}$ and $S_{\text{out}} = \{((J+1)l - 1)d, l = 1, 2, \ldots, L\}$. It is noted that NA is a receive processing technique originally introduced for passive sensing. In this paper, we discuss new transmit approach for NA in wideband MIMO system and explore the associated benefits in terms of DOF and DOA estimation.

3. Proposed techniques

In this section, we first present a new transmit scheme for wideband MIMO system. Then we illustrate how to further improve the DOF of the sum coarray using difference coarray processing. Finally, we show how to use the system mentioned above for DOA estimation.

3.1. Transmit scheme

Suppose that the transmit signals are chirps with $f_{\min}$ being the lowest frequency and B the bandwidth. To facilitate the separation of the signals transmitted from different antennas at the receiver, we split the chunk of bandwidth B into multiple non-overlapping sub-bands $B_1, B_2, \ldots, B_M$, each sub-band carrying a different chirp signal that is transmitted by one antenna during one pulse. A total of M pulses is employed to create cyclic transmissions among transmit antennas. Specifically, let B_m be the bandwidth which corresponds to the mth sub-band. During the transmission of the first pulse, the sub-band used by antenna 1 is B_1 and from antenna m is B_m. For the next pulse, B_{m+1} is used by antenna m, $m = 1, \ldots, M-1$ and band B_1 is used by antenna M. This transmit scheme is shown in Fig. 1 and Table 1 for the nested array MIMO system with 4 antennas.

Table 1
Sub-band Allocation for $M = 4$ antenna nested array Wideband MIMO system.

	Antenna 1	Antenna 2	Antenna 3	Antenna 4
Pulse 1	B_1	B_2	B_3	B_4
Pulse 2	B_2	B_3	B_4	B_1
Pulse 3	B_3	B_4	B_1	B_2
Pulse 4	B_4	B_1	B_2	B_3

Let $s_m(l, t)$ be the mth baseband signal transmitted by the mth antenna during the l th pulse. The transmitted bandpass signal can be written as $\tilde{s}_m(l, t) = s_m(l, t)e^{j2\pi f_c t}$, where f_c denotes the center frequency of the carrier. For a target located at location $\theta_k, k = 1, \ldots, K$, with K being the number of targets, the bandpass signal at the target after the lth pulse is given by

$$\tilde{x}(l, t) = \sum_{m=0}^{M-1} \tilde{s}_m(l, t - t_{tx,m}(\theta_k)) \tag{1}$$

where $t_{tx,\,m}(\theta_k)$ is the time taken for the signal to travel from the mth transmit element to the kth target.

3.2. Receiver processing

At the receiver end, the received bandpass signal at the ith antenna after the lth pulse is given by

$$\tilde{y}_i(l, t) = \sum_{k=1}^{K} \beta_k \tilde{x}(l, t - t_{rx,i}(\theta_k)) + \tilde{n}_i(l, t) \tag{2}$$

where β_k is the complex reflection coefficient of the kth target, $\tilde{n}_i(l, t)$ denotes the bandpass noise, $t_{rx,\,i}(\theta_k)$ is the time taken for the signal to get back to the ith receive element. The corresponding baseband signal can be written as

$$\begin{aligned} y_i(l, t) = &\sum_{k=1}^{K} \sum_{m=0}^{M-1} \beta_k e^{-j2\pi f_c (t_{rx,i}(\theta_k) + t_{tx,m}(\theta_k))} \\ &\times s_m(l, t - t_{tx,m}(\theta_k) - t_{rx,i}(\theta_k)) + n_i(l, t) \end{aligned} \tag{3}$$

where $n_i(l, t)$ denotes the baseband noise. Let antenna one be the reference antenna. Then, we can write

$$t_{tx,m}(\theta_k) = t_{tx,1}(\theta_k) + \tau_{tx,m}(\theta_k) \tag{4}$$

where $t_{tx,\,1}(\theta_k)$ denotes the propagation delay associated with the transmission from the reference antenna to the target, and $\tau_{tx,\,m}(\theta_k)$ the extra delay from the mth antenna to target. Note that the relative time delay $\tau_{tx,\,m}(\theta_k)$ is of interest in practice, since it contains the angle information of the target. Thus, we can compensate for the delay $t_{tx,\,1}(\theta_k)$ in the received signals. To compensate

for the delay $t_{tx,1}(\theta_k)$ in the received signals, it is a standard practice in radar signal processing to divide the un-certainty region of the target range into a set of range bins, and target detection and estimation is performed on each range bin one by one. In this case, the delay associated with that range bin is known and can be used for delay compensation [12]. The same compensation is performed on $t_{rx,i}(\theta_k)$. Accordingly, $t_{tx,1}(\theta_k)$ and $t_{rx,1}(\theta_k)$ are eliminated by using the received signal at the reference antenna due to the transmission from the same antenna, and therefore the system model in time domain can be formulated as

$$\begin{aligned}\acute{y}_i(l,t) &= y_i(l,t+t_{tx,1}(\theta_k)+t_{rx,1}(\theta_k)) \\ &= \sum_{k=1}^{K}\sum_{m=0}^{M-1}\beta_k e^{-j2\pi f_c(\tau_{rx,i}(\theta_k)+\tau_{tx,m}(\theta_k))} \\ &\quad\times s_m(l,t-\tau_{tx,m}(\theta_k)-\tau_{rx,i}(\theta_k))+\acute{n}_i(l,t)\end{aligned} \tag{5}$$

For notational convenience, we drop the superscript in $\acute{y}_i(l,t)$ and $\acute{n}_i(l,t)$ and use the same symbols for the signals after the compensation instead.

After applying the Fourier transformation on (5), the received signal of the lth pulse can be written in the frequency domain as

$$\begin{aligned}Y_i(l,f_n) &= \sum_k \beta_k e^{-j2\pi(f_n+f_c)\tau_{rx,i}(\theta_k)}\sum_m e^{-j2\pi(f_n+f_c)\tau_{tx,m}(\theta_k)} \\ &\quad\times S_m(l,f_n)+N_m(l,f_n)\end{aligned} \tag{6}$$

with $f_n = f_{\min}+(n-1)B/(N-1), n=1,\ldots,N$ denotes the nth frequency component, and N is the number of frequency samples.

Define the nth frequency component of the transmitted signals during the lth pulse as

$$\mathbf{s}(l,f_n) = \begin{bmatrix}S_1(l,f_n) & S_2(l,f_n) & \cdots & S_M(l,f_n)\end{bmatrix}^{\mathrm{T}} \tag{7}$$

Recall the frequency division in the previous subsection, it is easy to show that $\mathbf{s}(l,f_n)$ is a vector of all zeros except a $S_m(l,f_n)$ at the mth position, where m is concurrently decided by the number of elements M, frequency samples N, pulse index l and frequency index n. Also define

$$\mathbf{y}(l,f_n) = \begin{bmatrix}Y_1(l,f_n) & Y_2(l,f_n) & \cdots & Y_M(l,f_n)\end{bmatrix}^{\mathrm{T}} \tag{8}$$

as the received signal vector at frequency f_n, and

$$\mathbf{n}(l,f_n) = \begin{bmatrix}N_1(l,f_n) & N_2(l,f_n) & \cdots & N_M(l,f_n)\end{bmatrix}^{\mathrm{T}} \tag{9}$$

the additive noise vector at frequency f_n. $\mathbf{n}(l,f_n)$ follows a Gaussian distribution by the central limit theorem and is usually assumed to be i.i.d Gaussian distribute with zero mean and covariance matrix $\sigma_n^2\mathbf{I}$ (see, e.g., [13]). The signal model in (6) can be rewritten using a vector notation as

$$\mathbf{y}(l,f_n) = \sum_{k=1}^{K}\beta_k\mathbf{a}_r(\theta_k,f_n)\mathbf{a}_t^{\mathrm{T}}(\theta_k,f_n)\mathbf{s}(l,f_n)+\mathbf{n}(l,f_n) \tag{10}$$

where

$$\mathbf{a}_r(\theta_k,f_n) = \begin{bmatrix}1 & e^{-j2\pi(f_n+f_c)\tau_{rx,2}(\theta_k)} & \cdots & e^{-j2\pi(f_n+f_c)\tau_{rx,M}(\theta_k)}\end{bmatrix}^{\mathrm{T}} \tag{11}$$

and

$$\mathbf{a}_t(\theta_k,f_n) = \begin{bmatrix}1 & e^{-j2\pi(f_n+f_c)\tau_{tx,2}(\theta_k)} & \cdots & e^{-j2\pi(f_n+f_c)\tau_{tx,M}(\theta_k)}\end{bmatrix}^{\mathrm{T}} \tag{12}$$

denote the $M\times 1$ receive and transmit steering vector at frequency f_n, respectively.

The received signal is processed by a matched filter in the frequency domain, which outputs

$$\mathbf{Y}(f_n) = \left[\sum_{l=1}^{M}\mathbf{y}(l,f_n)\mathbf{s}^{\mathrm{H}}(l,f_n)\right]\left[\sum_{l=1}^{M}\mathbf{s}(l,f_n)\mathbf{s}^{\mathrm{H}}(l,f_n)\right]^{-1} \tag{13}$$

Recall that the transmitted waveforms are chirps, we can obtain that $S_m(l,f_n)S_m^{\mathrm{H}}(l,f_n)=c$, where c is a constant. Combined with the pulse-wise frequency division as shown in Table 1, we have

$$\sum_{l=1}^{M}\mathbf{s}(l,f_n)\mathbf{s}^{\mathrm{H}}(l,f_n) = S_m(l,f_n)S_m^{\mathrm{H}}(l,f_n)\sum_{m=1}^{M}\mathbf{e}_m\mathbf{e}_m^{\mathrm{H}} = c\,\mathbf{I}$$

with $\mathbf{e}_m$ being a column vector of all zeros except a 1 at the mth position. As a result, $\mathbf{s}(l,f_n)$ can be removed from (13) as follows:

$$\mathbf{Y}(f_n) = \sum_{k=1}^{K}\beta_k\mathbf{a}_r(\theta_k,f_n)\mathbf{a}_t^{\mathrm{T}}(\theta_k,f_n)+\mathbf{N}(f_n) \tag{14}$$

where $\mathbf{N}(f_n)$ denotes the noise component after the matched filter, which can be easily shown to contain independent and identically distributed Gaussian entries with zero mean and covariance σ_n^2.

Vectorizing $\mathbf{Y}(f_n)$ leads to

$$\mathbf{y}(f_n) \triangleq \mathrm{vec}(\mathbf{Y}(f_n)) = \mathbf{A}_n\boldsymbol{\beta}+\mathbf{n}_n \tag{15}$$

where $\boldsymbol{\beta} = [\beta_1,\ldots,\beta_K]^{\mathrm{T}}$, $\mathbf{n}_n \triangleq \mathrm{vec}(\mathbf{N}(f_n))$, and $\mathbf{A}_n = [\mathbf{a}(\theta_1,f_n),\ldots,\mathbf{a}(\theta_K,f_n)]$, with $\mathbf{a}(\theta_k,f_n) = \mathbf{a}_t(\theta_k,f_n)\otimes\mathbf{a}_r(\theta_k,f_n)$ being the joint transmit-receive steering vector. Assume that the β_k's, which refers to the radar cross section (RCS) of the kth target, are uncorrelated for different k. The RCS depends on the size, shape, directivity/orientation, and material of the target. It is a standard assumption in the radar literature that the RCS's of different targets are uncorrelated [12]. In addition, the RCS is typically modeled as a zero-mean random variable with covariance σ_k^2 (see, e.g., [14,15]). The autocorrelation matrix of $\mathbf{y}_n$ is then given by

$$\mathbf{R}_n = E\left[\mathbf{y}(f_n)\mathbf{y}^{\mathrm{H}}(f_n)\right] = \mathbf{A}_n\mathrm{diag}(\mathbf{p})\mathbf{A}_n^{\mathrm{H}}+\sigma_n^2\mathbf{I} \tag{16}$$

where $\mathbf{p} \triangleq [\sigma_1^2,\ldots,\sigma_K^2]^{\mathrm{T}}$ denotes the equivalent source signal vector.

3.3. DOA estimation

1) An Incoherent Subspace Method (ISM): The proposed system can obtain additional DOF by difference coarray processing. Specifically, we vectorize $\mathbf{R}_n$ as follows:

$$\mathbf{r}_n = \mathrm{vec}(\mathbf{R}_n) = (\mathbf{A}_n^*\odot\mathbf{A}_n)\mathbf{p}+\sigma_n^2\mathbf{e} \tag{17}$$

where $\mathbf{e}\triangleq\mathrm{vec}(\mathbf{I})$. Note that the difference coarray manifold $\mathbf{B}_n \triangleq \mathbf{A}_n^*\odot\mathbf{A}_n$ is a matrix with redundancy. After removing the repeated rows and sorting, we get a filled virtual array with $N_{\mathrm{od}} = 4L(J+1)-3$ elements. Applying the same redundancy removal and sorting procedure to $\mathbf{r}_n$ yield

$$\mathbf{x}_n = \mathbf{B}_n'\mathbf{p}+\mathbf{e}_n' \tag{18}$$

where $\mathbf{B}_n'$ and $\mathbf{e}_n'$ are the corresponding $N_{\mathrm{od}}\times K$ virtual array manifold matrix and noise signal which includes contributions from the $\mathbf{e}$ vector. Then spatial smoothing can be used to form a covariance matrix by dividing the N_{od} element virtual array into $N_s = (N_{\mathrm{od}}+1)/2$ subarrays, each with N_s elements. Let the observation vector of the ith subarray be $\mathbf{x}_n^i$. The spatial smoothed covariance matrix $\mathbf{R}_n^{\mathrm{avg}}$ is given by

$$\mathbf{R}_n^{\mathrm{avg}} = \frac{1}{N_s}\sum_{i=1}^{N_s}\mathbf{x}_n^i\left(\mathbf{x}_n^i\right)^{\mathrm{H}} \tag{19}$$

Using $\mathbf{R}_n^{\mathrm{avg}}$ with the multiple signal classification (MUSIC) algorithm [10], we can obtain the DOA spectrum $M_n(\theta)$ at frequency f_n. Combining the resulting measurements for all frequencies, outputs the combined DOA spectrum, whose peak locations correspond to the estimated DOAs.

2) Coherent methods: It is known that coherent processing, which proceeds by transforming the wideband signals at multiple frequencies into one focusing frequency, can significantly improve the DOA estimation performance with better detection and resolution thresholds than its incoherent counterpart. In the following we extend the conventional coherent signal subspace method for the proposed nested array wideband MIMO system, and present two coherent DOA estimation methods which construct focusing matrices from the difference coarray of the MIMO virtual array.

The proposed methods consist of two steps. First, the measured signal subspace $\mathcal{S}_c(\mathbf{B}_n)$ is rotated and transformed into a focusing

subspace. Unlike traditional coherent methods which construct focusing matrices based on the physical array, we propose a focusing using the virtual array instead. Specifically, the modified total least-squares coherent signal-subspace based focusing method (MTLS) [16] is applied to the virtual array output in (17). The focusing matrix corresponding to the nth frequency is give by

$$\mathbf{T}(f_n) = \mathbf{B}_0\left(\mathbf{B}_0^{\mathrm{H}}\mathbf{B}_0\right)^{-(1/2)}\left(\mathbf{B}_n^{\mathrm{H}}\mathbf{B}_n\right)^{-(1/2)}\mathbf{B}_n^{\mathrm{H}} \tag{20}$$

where $\mathbf{B}_0$ is the virtual array manifold at the center frequency $f_0 = f_{\min} + B/2$. In practice, to determine $\mathbf{B}_0$ and $\mathbf{B}_n$, a preprocessing step is required, where the conventional MUSIC is applied to estimate the DOAs of the sources. Let $\mathbf{W}_0 = \mathbf{B}_0\left(\mathbf{B}_0^{\mathrm{H}}\mathbf{B}_0\right)^{-(1/2)}$ and $\mathbf{W}_n = \mathbf{B}_n\left(\mathbf{B}_n^{\mathrm{H}}\mathbf{B}_n\right)^{-(1/2)}$ be the unitary matrices of the polar decomposition of $\mathbf{B}_0$ and $\mathbf{B}_n$, respectively. The output model after the focusing is given by

$$\mathbf{z}_n = \mathbf{T}(f_n)\mathbf{r}_n = \mathbf{W}_0\mathbf{W}_n^{\mathrm{H}}\mathbf{B}_n\mathbf{p} + \sigma_n^2\mathbf{W}_0\mathbf{W}_n^{\mathrm{H}}\mathbf{e} \tag{21}$$

Averaging the output signal at each frequency according to [16] outputs the universal covariance matrix

$$\mathbf{R} = \mathbf{W}_0\left(\textstyle\sum_{n=1}^{N}\mathbf{W}_n^{\mathrm{H}}\mathbf{R}_{\mathbf{r}_n}\mathbf{W}_n\right)\mathbf{W}_0^{\mathrm{H}} \tag{22}$$

where $\mathbf{R}_{\mathbf{r}_n} = E[\mathbf{r}_n\mathbf{r}_n^{\mathrm{H}}]$. Recall that $\mathbf{B}_0$ is a matrix with redundancy, and so is $\mathbf{R}$. Applying similar redundancy removal and sorting procedure as shown in (17)–(19) to $\mathbf{R}$ outputs a $N_s \times N_s$ spatial smoothed covariance matrix, which we denote by $\mathbf{R}_0$. In practice, the autocorrelation matrix $\mathbf{R}_n$ is generally estimated from the sample correlation matrix using T snapshots

$$\hat{\mathbf{R}}_n = \tfrac{1}{T}\textstyle\sum_{t=1}^{T}\mathbf{y}(f_n,t)\mathbf{y}^{\mathrm{H}}(f_n,t) \tag{23}$$

Some structured covariance matrix estimators [17,18] can also be employed to enhance the DOA estimation performance. If we start from $\hat{\mathbf{R}}_n$ instead of $\mathbf{R}_n$ defined in (16), then the quantities $\mathbf{r}_n$ (17), $\mathbf{z}_n$ (21), $\mathbf{R}_{\mathbf{r}_n}$ and $\mathbf{R}$ in (22), and $\mathbf{R}_0$ are replaced with the finite snapshot versions $\hat{\mathbf{r}}_n$, $\hat{\mathbf{z}}_n$, $\hat{\mathbf{R}}_{\mathbf{r}_n}$, $\hat{\mathbf{R}}$ and $\hat{\mathbf{R}}_0$, which are used hereinafter.

The eigen decomposition of $\hat{\mathbf{R}}_0$ is given by

$$\hat{\mathbf{R}}_0 = \textstyle\sum_{i=1}^{N_s}\lambda_i\mathbf{e}_i\mathbf{e}_i^{\mathrm{H}} = \hat{\mathbf{U}}_S\hat{\mathbf{\Sigma}}_S\hat{\mathbf{U}}_S^{\mathrm{H}} + \hat{\mathbf{U}}_N\hat{\mathbf{\Sigma}}_N\hat{\mathbf{U}}_N^{\mathrm{H}} \tag{24}$$

where λ_i and $\mathbf{e}_i$ denote the ith eigenvalue and eigenvector, respectively. $\hat{\mathbf{U}}_S$ and $\hat{\mathbf{U}}_N$ are defined as the signal subspace and noise subspace, respectively. $\hat{\mathbf{\Sigma}}_S$ and $\hat{\mathbf{\Sigma}}_N$ are diagonal matrices with the eigenvalues associated with the signal subspace and noise subspace, respectively, on their diagonal. Also define $\mathbf{\Phi}_0 = [\boldsymbol{\phi}(\theta_1), \ldots, \boldsymbol{\phi}(\theta_K)]$ as the $N_s \times K$ effective array manifold, where $\boldsymbol{\phi}(\theta_k) = [1, \ldots, \exp\{-j2\pi(N_s-1)d\sin(\theta_k)/\lambda\}]^{\mathrm{T}}$, with λ being the wavelength at the focusing frequency. The spectrum of the proposed MTLS-MUSIC method can then be formulated as

$$P(\theta) = \frac{1}{\boldsymbol{\phi}^{\mathrm{H}}(\theta)\hat{\mathbf{U}}_N\hat{\mathbf{U}}_N^{H}\boldsymbol{\phi}(\theta)} \tag{25}$$

Compared to MUSIC, weighted subspace fitting (WSF) is known to give low estimation error that asymptotically attains the stochastic Cramér-Rao bound [19]. Alternatively, we can estimate the DOA using (24) from a WSF perspective. Specifically, the signal subspace fitting problem can be formulated as

$$\hat{\boldsymbol{\theta}}_{\mathrm{SF}}, \hat{\mathbf{P}} = \arg\min_{\boldsymbol{\theta}}\left\|\hat{\mathbf{U}}_S\hat{\mathbf{W}}^{1/2} - \mathbf{\Phi}_0(\boldsymbol{\theta})\mathbf{P}\right\|_F^2 \tag{26}$$

where $\mathbf{P}$ is a $K\times K$ matrix of full rank. $\hat{\mathbf{W}}$ is a $K\times K$ weighting matrix whose optimal value is given by $\hat{\mathbf{W}}_{\mathrm{opt}} = (\hat{\mathbf{\Sigma}}_S - \hat{\sigma}^2\mathbf{I})^2\hat{\mathbf{\Sigma}}_S^{-1}$, where $\hat{\sigma}^2$ can be estimated from the $N_s - K$ smallest eigenvalues of $\hat{\mathbf{R}}_0$. By solving for $\hat{\mathbf{P}}$ iteratively and substituting back in (26), the estimated DOA $\hat{\boldsymbol{\theta}}_{\mathrm{SF}}$ can be obtained.

Note that WSF needs an accurate initialization which is not easy to obtain, we then extend the sparse recovery method based on weighted subspace fitting (SRWSF) [20] for the proposed nested array wideband MIMO sensing system. Define $\mathbf{\Phi} = [\boldsymbol{\phi}(\tilde{\theta}_1), \ldots, \boldsymbol{\phi}(\tilde{\theta}_{N_g})]$ as an overcomplete basis matrix, where $\mathbf{\Theta} = [\tilde{\theta}_1, \tilde{\theta}_2, \ldots, \tilde{\theta}_{N_g}]$ denotes a dense grid that samples the potential spatial scope of incident signals by N_g points and assume that the true DOAs belong to $\mathbf{\Theta}$. Then the MTLS-SRWSF method for the nested array wideband system can be formulated as

$$\hat{\tilde{\mathbf{P}}} = \arg\min_{\tilde{\mathbf{P}}}||\tilde{\mathbf{P}}||_{2,1}, \quad s.t. \quad ||\hat{\mathbf{U}}_S\hat{\mathbf{W}}_{\mathrm{opt}}^{1/2} - \mathbf{\Phi}\tilde{\mathbf{P}}||_F \le \beta \tag{27}$$

where $||\tilde{\mathbf{P}}||_{2,1} \triangleq \sum_{i=1}^{N_g}||\tilde{\mathbf{P}}_i||$, and $\tilde{\mathbf{P}} = [\tilde{\mathbf{P}}_1^{\mathrm{T}}, \ldots, \tilde{\mathbf{P}}_{N_g}^{\mathrm{T}}]^{\mathrm{T}}$ is a row sparse matrix, whose non-zero rows correspond to the true DOAs. β is a regulation parameter, which is selected as in [19]. Note that (27) can be reformulated as a second-order cone program, which can be solved by standard convex optimization packages. The DOAs of the multiple sources can be estimated by locating the peaks of a spatial pseudo-spectrum of $\tilde{\mathbf{P}}$.

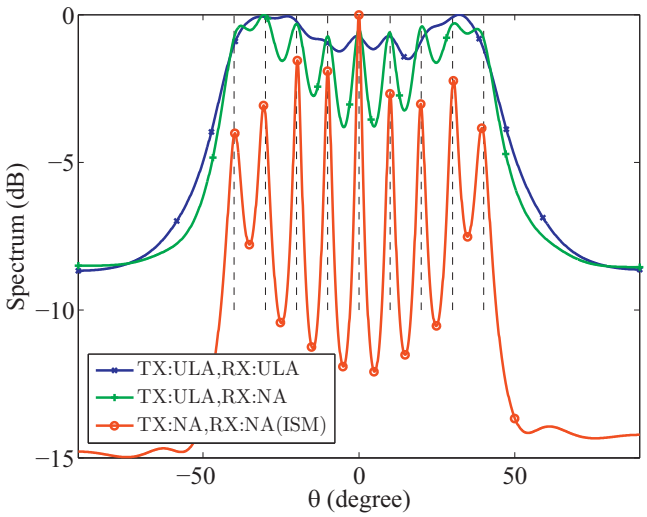

Fig. 2. MUSIC spatial spectrum of $K = 9$ sources under 3 different array configurations.

4. Numerical results

To illustrate the benefits of using the proposed transmit scheme with NA in the wideband MIMO system, we compare 3 array configurations: (a) ULA for both transmit (TX) and receive (RX); (b) ULA for TX and, NA for RX; (c) NA for both TX and RX. For each configuration, we have $M = 4$ antennas with half wavelength separation between two adjacent elements for both the ULA and the inner array of the NA. For all configurations, $f_{\min} = 100$ Hz and $B = 5.9$ kHz. For MTLS-MUSIC and MTLS-SRWSF, the center frequency is selected as the focusing frequency. For all simulations, rank-constrained maximum likelihood (RCML) estimator proposed in [17] is used to estimate the autocorrelation matrix $\mathbf{R}_n$.

First, we consider a case with 9 targets located at $(-40^\circ, -30^\circ, -20^\circ, -10^\circ, 0^\circ, 10^\circ, 20^\circ, 30^\circ, 40^\circ)$. The signal-to-noise ratio (SNR) is set to 0 dB. Fig. 2 depicts the MUSIC spectrum of all 3 configurations, while Fig. 3 shows the MTLS-MUSIC and MTLS-SRWSF spectrum for Configuration (c). It is easy to show that the DOF is $L(J+1)+M-1$ for Configuration (b) and $2L(J+1)-1$ for Configuration (c), or 9 and 11, respectively. It is seen from Fig. 2 that Configurations (a) and (b) fail to resolve all 9 targets because the number of sources has exceeded their capability. Meanwhile, Configuration (c) which employs NA for both TX and RX with additional DOF, can adequately resolve all 9 sources. It is also noted that the peaks of MTLS-SRWSF and MTLS-MUSIC are sharper and narrower than others. MTLS-SRWSF is observed to have a higher peak-to-sidelobe ratio but with pseudo peaks

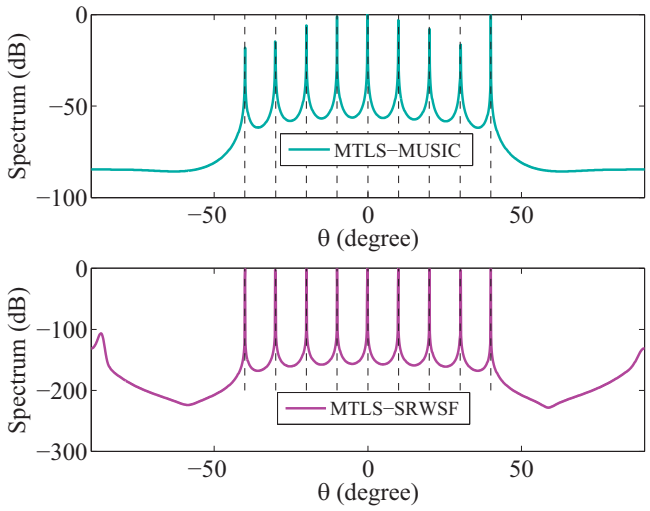

Fig. 3. Spatial spectrum of $K = 9$ sources for MTLS-MUSIC and MTLS-SRWSF under Configuration (c).

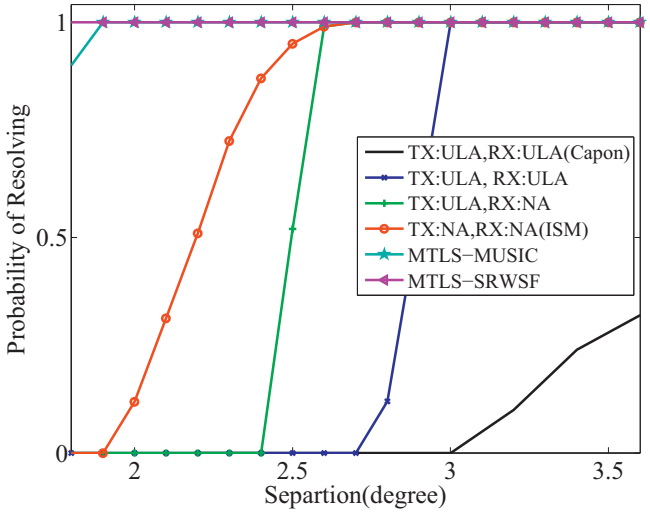

Fig. 4. Probability of success of two sources versus the DOA separation.

caused by inaccurate initialization, indicating that MTLS-SRWSF is capable of a better DOA accuracy but is also more sensitive to the initialization in the focusing procedure.

Next, we consider the resolution of the considered schemes. In Figs. 4 and 5, we respectively plot the probability of success in resolving two closely spaced sources and average root mean square error (RMSE) of the DOA estimates $\hat{\theta}_1$ and $\hat{\theta}_2$ versus the angle separation $\Delta\theta \triangleq |\theta_2 - \theta_1|$, averaged over $Q = 100$ Monte Carlo runs. For each simulation, the two sources are considered successfully resolved if the larger of the two estimation errors, $|\hat{\theta}_1 - \theta_1|$ and $|\hat{\theta}_2 - \theta_2|$, is smaller than $0.5\Delta\theta$. For better comparison, the Capon method [21,22] with a regular ULA configuration was included in Figs. 4 and 5 to serve as a benchmark of the DOF and DOA accuracy. Clearly the proposed transmit scheme with NA for both TX and RX outperforms the other two configurations. Specifically for Configuration (c), both MTLS-MUSIC and MTLS-SRWSF shows better precision than the ISM method at small angle separations.

5. Conclusion

We presented a new transmit scheme using cyclic transmission for wideband MIMO system with a colocated nested array, which separates the transmitted waveforms in the frequency domain, and allows the formation of a sum coarray. Based on the proposed scheme, two coherent DOA estimation methods which construct focusing matrices from the difference coarray of the MIMO virtual array were presented to take full advantage of the degrees of freedom (DOF) and improve the accuracy of DOA estimation. It is shown via simulation that the proposed methods yield improved accuracy than other methods at small angle separations.

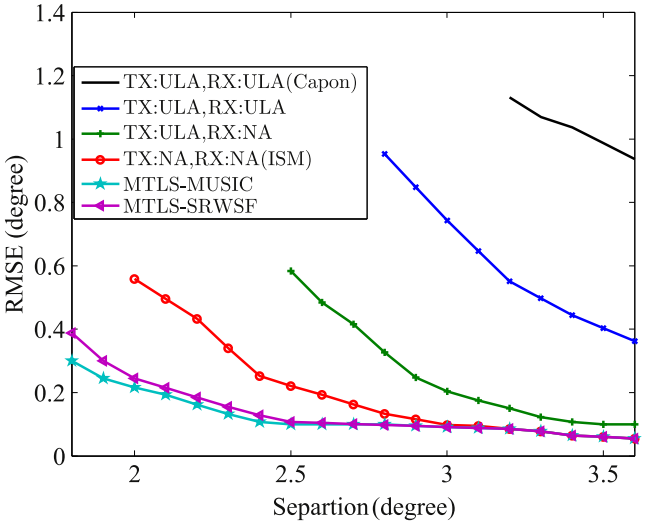

Fig. 5. RMSE of two sources versus the DOA separation.

References

[1] J. Li, P. Stoica, MIMO Radar with colocated antennas, IEEE Signal Process. Mag. 24 (5) (2007) 106–114.
[2] P. Stoica, J. Li, Y. Xie, On probing signal design for MIMO radar, IEEE Trans. Signal Process. 55 (8) (2007) 4151–4161.
[3] D.R. Fuhrmann, G. San Antonio, Transmit beamforming for MIMO radar systems using signal cross-correlation, IEEE Trans. Aerosp. Electron. Syst 44 (1) (2008).
[4] G. Hua, S.S. Abeysekera, MIMO radar transmit beampattern design with ripple and transition band control, IEEE Trans. Signal Process. 61 (11) (2013) 2963–2974.
[5] A. Aubry, A. De Maio, Y. Huang, MIMO radar beampattern design via PSL/ISL optimization, IEEE Trans. Signal Process. 64 (15) (2016) 3955–3967.
[6] G. Cui, X. Yu, V. Carotenuto, L. Kong, Space-time transmit code and receive filter design for colocated MIMO radar, IEEE Trans. Signal Process. PP (99) (2016). 1–1.
[7] P. Vaidyanathan, P. Pal, C.Y. Chen, MIMO radar with broadband waveforms: smearing filter banks and 2d virtual arrays, in: Proc. 42nd Asilomar Conf. Signals, Syst., Comput., IEEE, 2008, pp. 188–192.
[8] Y. Jin, X. Liu, J. Huang, Wideband transmit beampattern design for MIMO array, in: Proc. 2011 IEEE Int. Conf. Signal Process., Commun. Comput. (ICSPCC), IEEE, 2011, pp. 1–4.
[9] O. Gómez, F. Nadal, P. Jardin, G. Baudoin, B. Poussot, On wideband MIMO radar: Detection techniques based on a DFT signal model and performance comparison, in: Proc. IEEE Radar Conf., IEEE, 2012, pp. 0608–0612.
[10] P. Pal, P. Vaidyanathan, Nested arrays: a novel approach to array processing with enhanced degrees of freedom, IEEE Trans. Signal Process. 58 (8) (2010) 4167–4181.
[11] L. Mao, H. Li, Q. Zhang, Transmit subaperturing for MIMO radars with nested arrays, Signal Process. 134 (2017) 244–248.
[12] M.I. Skolnik, Introduction to Radar Systems, third ed., McGraw-Hill, New York, NY, USA, 2001.
[13] J.C. Chen, R.E. Hudson, K. Yao, Maximum-likelihood source localization and unknown sensor location estimation for wideband signals in the near-field, IEEE Trans. Signal Process. 50 (8) (2002) 1843–1854.
[14] M.A. Richards, Fundamentals of Radar Signal Processing, McGraw-Hill, New York, NY, USA, 2005.
[15] E. Fishler, A. Haimovich, R.S. Blum, L.J. Cimini, D. Chizhik, R.A. Valenzuela, Spatial diversity in radars–models and detection performance, IEEE Trans. Signal Process. 54 (3) (2006) 823–838.
[16] S. Valaee, B. Champagne, P. Kabal, Localization of wideband signals using least-squares and total least-squares approaches, IEEE Trans. Signal Process. 47 (5) (1999) 1213–1222.
[17] B. Kang, V. Monga, M. Rangaswamy, Rank-constrained maximum likelihood estimation of structured covariance matrices, IEEE Trans. Aerosp. Electron. Syst 50 (1) (2014) 501–515.

[18] A. Aubry, A. De Maio, L. Pallotta, A geometric approach to covariance matrix estimation and its applications to radar problems, IEEE Trans. Signal Process. 66 (4) (2018) 907–922.
[19] M. Viberg, B. Ottersten, T. Kailath, Detection and estimation in sensor arrays using weighted subspace fitting, IEEE Trans. Signal Process. 39 (11) (1991) 2436–2449.
[20] N. Hu, Z. Ye, D. Xu, S. Cao, A sparse recovery algorithm for DOA estimation using weighted subspace fitting, Signal Process. 92 (10) (2012) 2566–2570.
[21] T.L. Marzetta, A new interpretation of capon's maximum likelihood method of frequency-wavenumber spectral estimation, IEEE Trans. Acoust. Speech Signal Process. 31 (2) (1983) 445–449.
[22] A. Aubry, V. Carotenuto, A. De Maio, A new optimality property of the capon estimator, IEEE Signal Process. Lett. PP (99) (2017). 1–1.